

1 **Bioreactor with electrically deformable curved membranes for**
2 **mechanical stimulation of cell cultures**

3 **Joana Costa^{1,2}, Michele Ghilardi^{3,4}, Virginia Mamone^{2,5}, Vincenzo Ferrari^{2,5}, James J.C.**
4 **Busfield^{3,4}, Arti Ahluwalia^{1,2}, Federico Carpi^{6*}**

5 ¹Research Center "E. Piaggio", University of Pisa, Pisa, Italy

6 ²Department of Information Engineering, University of Pisa, Pisa, Italy

7 ³School of Engineering And Materials Science, Queen Mary University of London, London, UK

8 ⁴Materials Research Institute, Queen Mary University of London, London, UK

9 ⁵EndoCas Center for computer-assisted surgery, University of Pisa, Pisa, Italy

10 ⁶Department of Industrial Engineering, University of Florence, Florence, Italy

11 ***Correspondence:**

12 Federico Carpi

13 federico.carpi@unifi.it

14 **Keywords:** actuator, bioreactor, cell, dielectric elastomer, electroactive polymer, mechanical
15 stimulation, membrane, stretch

16 **Number of words:** 3882

17 **Number of figures:** 4

18 **Abstract**

19 Physiologically relevant in vitro models of stretchable biological tissues, such as muscle, lung,
20 cardiac and gastro-intestinal tissues, should mimic the mechanical cues which cells are exposed to in
21 their dynamic microenvironment in vivo. In particular, in order to mimic the mechanical stimulation
22 of tissues in a physiologically relevant manner, cell stretching is often desirable on surfaces with
23 dynamically controllable curvature. Here, we present a device that can deform cell culture
24 membranes without the current need for external pneumatic/fluidic or electrical motors, which
25 typically make the systems bulky and difficult to operate. We describe a modular device that uses
26 elastomeric membranes, which can intrinsically be deformed by electrical means, producing a
27 dynamically tuneable curvature. This approach leads to compact, self-contained, lightweight and
28 versatile bioreactors, not requiring any additional mechanical equipment. This was obtained via a
29 special type of dielectric elastomer actuator. The structure, operation and performance of early
30 prototypes are described, showing preliminary evidence on their ability to induce changes on the
31 spatial arrangement of the cytoskeleton of fibroblasts dynamically stretched for 8 hours.

32

33

34 1 Introduction

35 All biological tissues are subjected to internal mechanical forces that arise from interstitial flows and
36 cellular motions. These forces can redistribute effector molecules that are secreted by cells, resulting
37 in the coupling of chemical and mechanical signalling. This phenomenon, known as
38 mechanotransduction, is a major research interest in the fields of regenerative medicine and tissue
39 engineering (Griffith et al. 2006).

40 Static or cyclic and axial or biaxial strains applied to monolayers of cells, cultured on deformable
41 membranes or 3D scaffolds (Elsaadany et al. 2017), have been used for decades (Meikle et al. 1979;
42 Leung et al. 1977) to show that mechanical stretch can induce cell proliferation, increase tissue
43 organization and enhance mechanical properties of cultured tissues. At present, most of the
44 commercially available devices for cell stretching in vitro are actuated by pneumatic systems, such as
45 those from Flexcell® (Flexcell International, 2019), or mechanical motors, such as those from
46 Strex® (Strex, 2019). They require external driving units (vacuum pumps or motors), which make
47 the systems bulky, complex to operate, acoustically noisy and generally capable of low throughput
48 (Brown 2000).

49 Other systems are designed to mechanically stimulate cells at the microscopic scale, so as to study
50 the response of few or even single cells, with so-called organ-on-a-chip devices (Akbari and Shea
51 2012,a; Akbari and Shea 2012,b; Clark et al. 2000; Kim et al. 2012; Pavesi et al. 2015). They are
52 based on microfluidic systems, which advantageously host cells in highly miniaturised chambers,
53 although they are still limited by the need for much bulkier external fluidic components.

54 In order to obtain more compact and easier-to-use systems, the potential usage of smart materials (not
55 requiring external pumps/motors) is of growing interest. In particular, within the family of
56 electromechanically active polymers (Carpi 2016), dielectric elastomer actuators (DEAs) at present
57 can in general offer large strains (10-100%) and relatively high stresses (up to 1 MPa) in response
58 electrical stimuli, with simple structure, compact size, light weight and low power consumption
59 (Carpi et al. 2008; Pelrine et al. 2000). Due to these attractive properties, their potential also for the
60 mechano-stimulation of cells has recently been explored (Imboden et al. 2019; Poulin et al. 2018;
61 Poulin et al. 2016; Cei et al. 2016; Akbari and Shea 2012,a; Akbari and Shea 2012,b). However, so
62 far, they have been used for cell stretching of planar (uni- or bi-directional, or radial) and uniform
63 kind. As a difference, tissues in vivo mostly undergo stretch fields that are non-planar, anisotropic
64 and inhomogeneous (Balestrini et al. 2010). So, the greatest potential of these smart materials to
65 mimic physiologically-relevant conditions remains at present mostly unexplored.

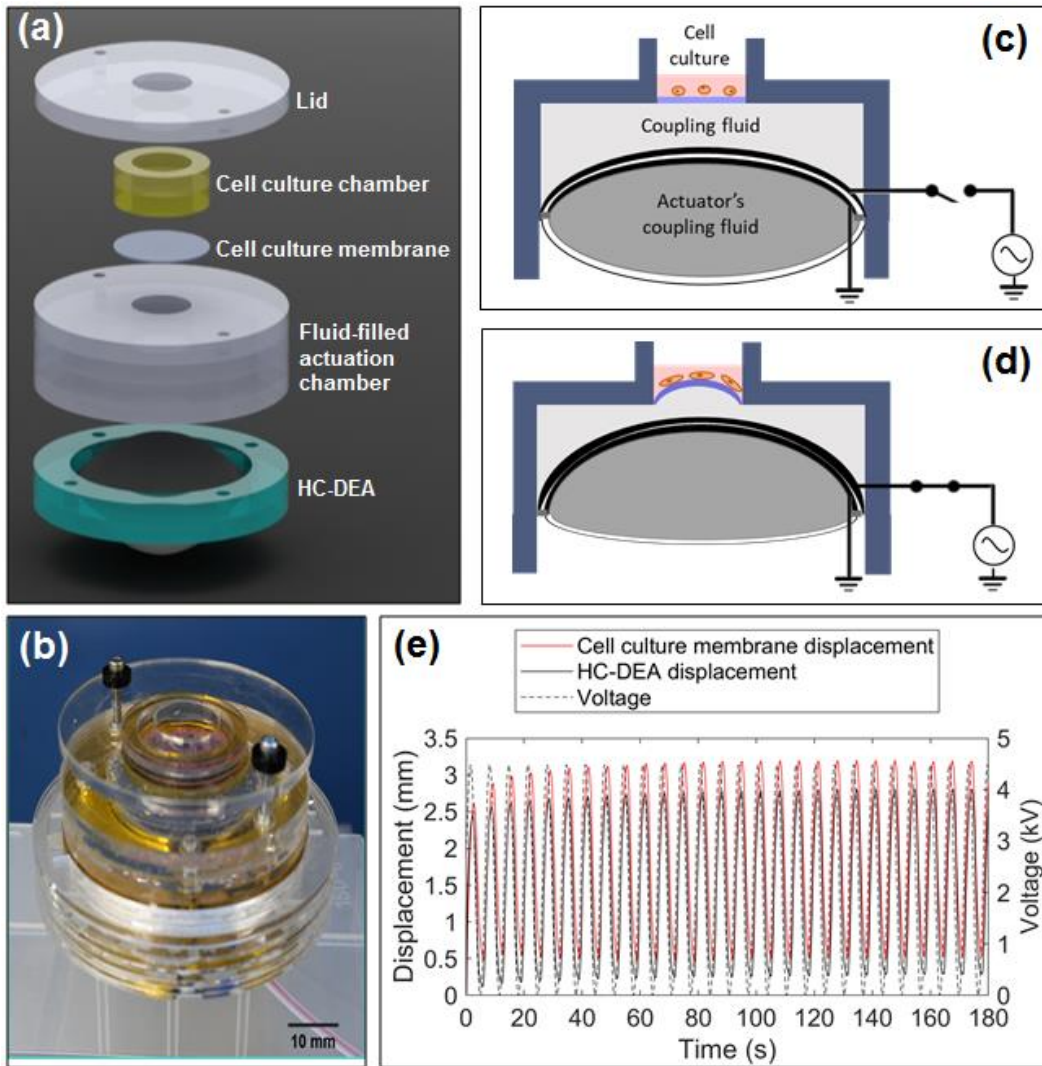
66 Here, we target a mechanical stimulation of cellular cultures on surfaces having a dynamically
67 controllable curvature. As an alternative to conventional hydraulic/fluidic systems that can achieve an
68 analogous effect, we present a DEA-based modular device made of elastomeric membranes that are
69 deformable electrically (i.e. their curvature can be dynamically tuned by purely electrical means),
70 without any fluidic system. This new approach is shown to lead to compact, self-contained and noise-
71 free bioreactors that do not require any additional external mechanical equipment, as detailed below.

72 2 Methods

73 The structure of the proposed bioreactor and its principle of operation are presented in Figures 1a,b.
74 An elastomeric cell culture membrane is arranged on top of a fluid-filled chamber that contains also a
75 soft actuator. With respect to conventional hydraulic/fluidic systems, the fluid here has a different
76 function, as explained below. The cell culture membrane seals the chamber and is in contact with the

77 fluid. When the actuator is off (no applied voltage), the membrane surface can either be flat or, if
 78 needed, have an initial pre-curvedness (obtained by increasing the fluid volume). In response to an
 79 applied voltage, the actuator is able to vary the cell culture membrane's curvature, according to a
 80 variable displacement of the fluid confined underneath, as detailed below.

81



82

83 **Figure 1.** Proposed bioreactor with electrically deformable curved membrane: (a) exploded view of
 84 the structure; (b) picture of an assembled prototype; (c),(d) schematic representation of the principle
 85 of operation; (e) examples of displacement signals (culture membrane and actuator) in response to a
 86 cyclic voltage.

87

88 The soft actuator consists of a special type of DEA, known as hydrostatically coupled dielectric
 89 elastomer actuator (HC-DEA) (Carpi et al. 2010). It is obtained by combining two dielectric
 90 elastomer circular films together and confining a coupling fluid between them, so as to obtain a
 91 bubble-like shape. One membrane (the one at the top in Figure 1c) is made active by sandwiching it
 92 between two compliant electrodes connected to a voltage source, while the other membrane (the one

93 at the bottom in Figure 1c) is passive. When a voltage is applied to the active membrane, the bubble-
94 like structure of the actuator deforms upwards (Figure 1d). This is due to an electrically induced
95 reduction of the active membrane's thickness and an increase in its area, while the passive membrane
96 buckles in the same direction as a result of the fluid-mediated coupling (Carpi et al.2010).

97 This electrically induced deformation of the actuator is then used to displace the second coupling
98 fluid confined above it (Figure 1d), so that the cell culture membrane can assume a controllable
99 curvature, depending on the magnitude of the applied voltage. It is worth noting that voltages of
100 opposite polarity and same amplitude cause the same curvature, as the actuation pressure generated
101 by the HC-DEA is dependent on the square of the applied voltage (Carpi et al. 2010), as for any other
102 DEA (Carpi et al. 2008). It is also useful to remark that the actuator's structure could easily be
103 modified by making both of its membranes active (i.e. providing both of them with electrodes) and
104 independently controllable, so as to make it able to buckle in both directions: this would enable bi-
105 directional displacements of the cell culture membrane, in order to obtain both tuneable convexities
106 and tuneable concavities.

107 According to this principle of operation, a voltage (either static or dynamic) applied to the soft
108 actuator can be used to generate a deformation of the cell culture membrane, stretching any adhered
109 cells both circumferentially and radially.

110 Prototypes of this device were manufactured as follows. For the actuator's active and passive
111 membranes, a 1mm-thick acrylic-based elastomeric film (VHB™ 4910, 3M, USA) was biaxially pre-
112 strained by 250% (i.e. 3.5 times pre-stretched), reaching an estimated thickness of about 82 μm , and
113 fixed to a plastic circular frame with an internal diameter of 50 mm. The active membrane's
114 compliant electrodes were manufactured using a custom-made conductive ink, consisting of a
115 dispersion of 9 wt% carbon black (Black Pearls 2000, Cabot, USA) in a silicone pre-polymer
116 (MED4901, NuSil, USA) dissolved in isooctane (Sigma Aldrich) with a 1:1 volume ratio. The
117 reagents were mixed using a planetary mixer (THINKY ARE-250, Intertronics, UK) and the
118 resulting ink was sprayed with an airbrush onto the active membrane's surfaces, where the silicone
119 matrix was cured, obtaining elastomeric electrodes.

120 The actuator was then assembled by pulling the passive membrane with a custom-build vacuum
121 chamber, filling the resulting cavity with 15 ml of a fluid silicone pre-polymer (Transil 40,
122 Mouldlife, UK) and finally closing the cavity with the active membrane. The adhesive properties of
123 the VHB elastomeric film allowed for sufficient bonding. The two membranes and the fluid
124 encapsulated between them formed a bubble-like structure, with the fluid acting as a hydrostatic
125 coupling medium between the membranes.

126 The cell culture membrane was manufactured by film casting with a silicone elastomer (Silbione
127 LSR 4305, BlueStar Silicones, Norway). It had a thickness of about 75 μm and a diameter of 16.5
128 mm. A fluid-mediated hydrostatic coupling was also established between the actuator and the cell
129 culture membrane, so as to transfer motion from the former to the latter. For simplicity, the adopted
130 fluid was the same silicone pre-polymer used inside the actuator. The cell culture chamber was fixed
131 to the rest of the structure with screws, so as to simplify the interchangeability among different types
132 of chambers, enabling system modularity.

133 The diameter of the cell culture membrane was smaller than that of the actuator. Therefore, the fluid
134 mediated coupling between surfaces of different area resulted in a larger vertical displacement in the
135 cell culture membrane with respect to that of the actuator. This effect (maximised by an

136 incompressible fluid) is evident from the sample signals shown in Figure 1e. Hence, changing the
 137 size of the cell culture membrane could be used to change the maximum achievable curvature at the
 138 maximum voltage, for any given actuator size. Moreover, for any given size of the cell culture
 139 membrane, the achievable curvature can always be modulated via the applied voltage.

140 A preliminary characterisation of prototypes of this new device is presented below.

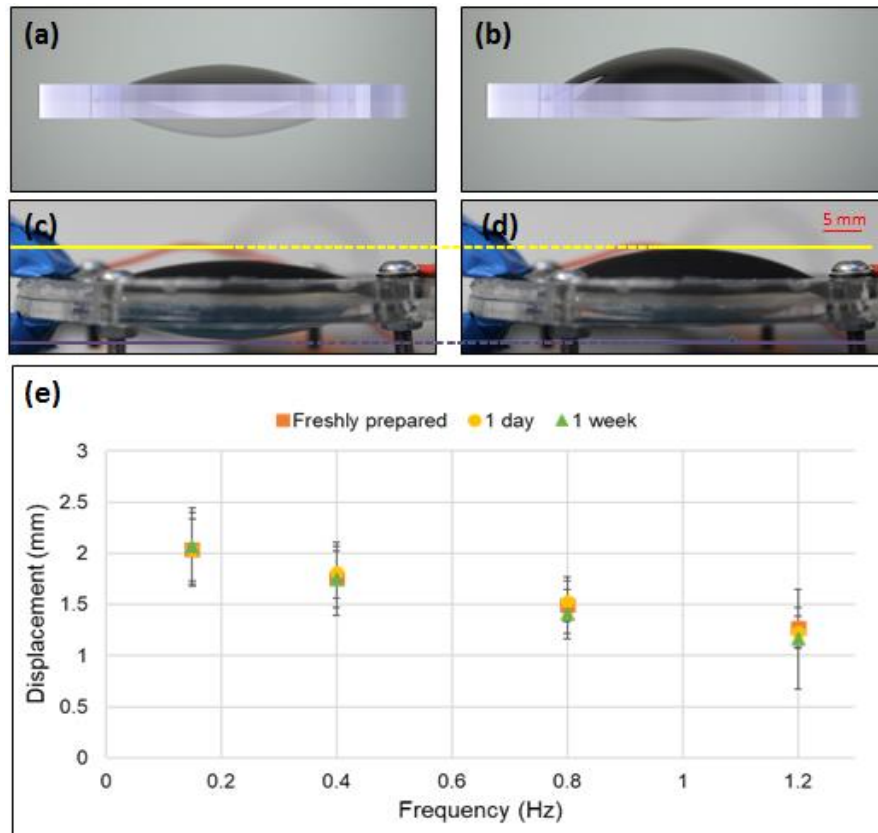
141

142 **3 Results and Discussion**

143 **3.1 Frequency response over time**

144 The HC-DEA dynamic performance was tested by measuring, with a laser-based displacement
 145 transducer (optoNCDT 1800, Micro-Epsilon, Germany), the active membrane’s maximum
 146 displacement (Figure 2a-d) in response to unipolar sinusoidal voltages.

147



148

149 **Figure 2.** Operation of the HC-DEA and its frequency response. The drawings (a),(b) and pictures
 150 (c),(d) of the device show it at electrical rest (a),(c) and with an applied voltage of 4.5 kV (b),(d).
 151 Panel (e) presents the frequency response to 4.5 kV sinusoidal waves in terms of maximum
 152 displacement of the central (highest) point of the active membrane, as measured at different times
 153 after fabrication: 0, 1 and 7 days. Error bars represent the standard deviation among three samples.

154

155 As these tests were aimed at assessing the frequency response and how it changes over time, the
156 amplitude of the voltage signals was fixed (4.5 kV, according to the thickness of the active
157 membrane) and the frequency was varied within the 0.15-1.2 Hz range, corresponding to
158 characteristic frequencies of intestinal, lung and cardiac tissue motions (Saul 1990; Taylor and
159 Eckberg 1996; Han et al. 1998). The signals were obtained from a custom-made generator based on a
160 miniature high voltage multiplier (Q50, EMCO High Voltage Corporation, USA). For each tested
161 frequency, the voltage signal was applied for 3 minutes, followed by 1 minute of rest. The
162 experiments were performed right after fabrication and then repeated after 1 and 7 days.

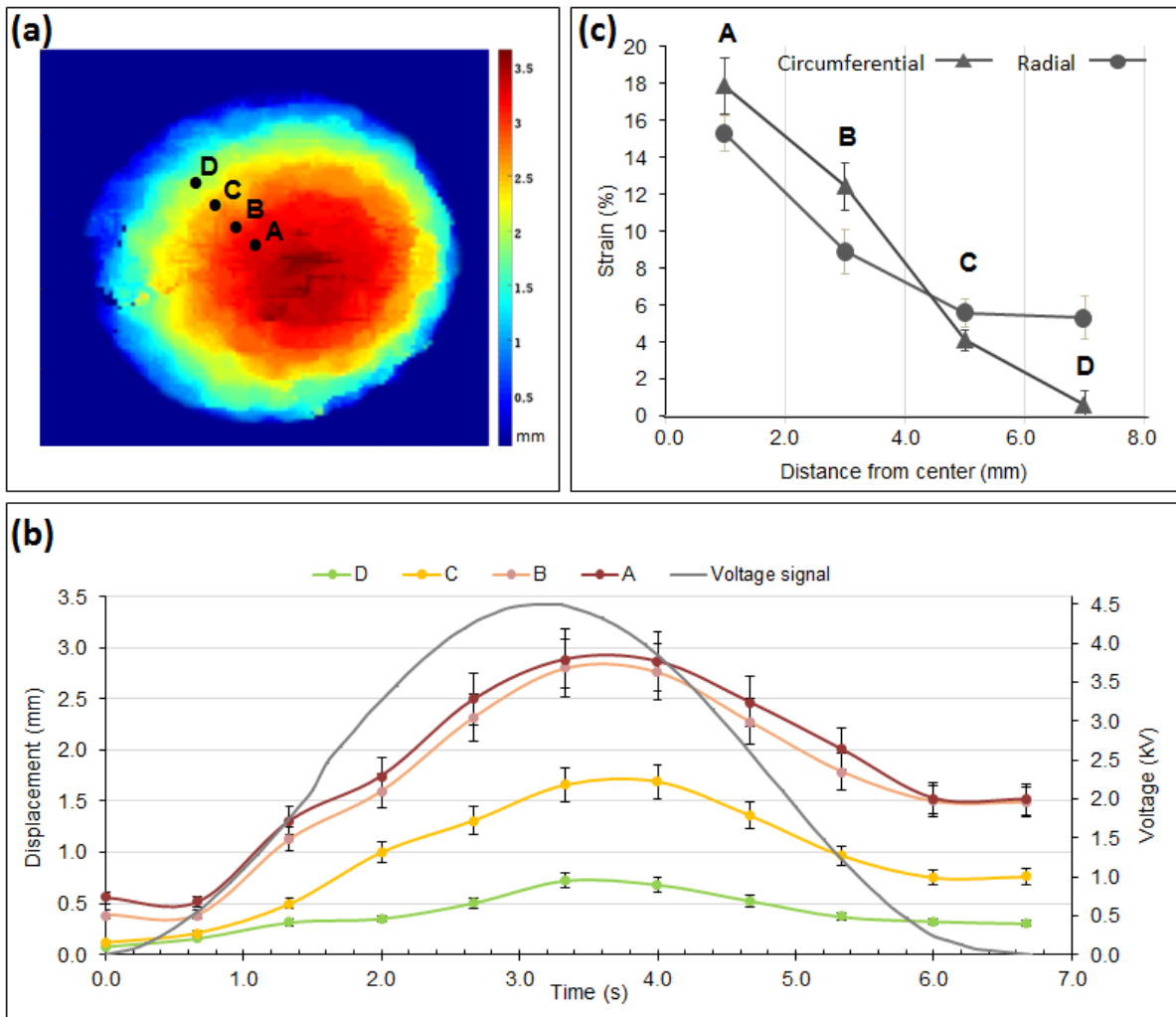
163 Figure 2e presents the results, showing that, as expected, there was a notable decrease of the
164 achievable displacement as the frequency increased. This can be ascribed to the viscous components
165 of the constitutive elastomeric membrane (Carpi et al. 2008). Nevertheless, for each frequency, the
166 average displacement was found to be stable over time, at least over the 7 days investigated (Figure
167 2e). This makes the technology potentially usable for continuous cell stretching over several days.

168 **3.2 Vertical displacements and radial and circumferential strains**

169 In order to investigate the deformation occurring in different regions of the cell culture membrane
170 and thus assess the mechanical stimuli imposed to cells adhered over its surface, the following tests
171 were performed.

172 The bioreactor was driven with a sinusoidal voltage of 4.5 kV at a frequency of 0.15 Hz and the bi-
173 dimensional distribution of the vertical displacement (displacement field map) and mono-
174 dimensional (radial) distribution of both the radial and circumferential strains were estimated.

175 Specifically, the displacement field map was defined as the spatial distribution of the maximum
176 vertical displacement (during one actuation cycle) of the cell culture membrane across its surface. It
177 was determined using a 3D optical mapping system based on two stereo cameras (LI-OV580-Stereo,
178 Leopard Imaging, USA) that captured images at regular time steps, when the bioreactor was at rest
179 and under electrical actuation. Figure 3a presents the resulting map, showing that the highest
180 displacements occurred, as expected, in the central region, reaching about 3 mm. Figure 3b presents
181 the time evolution of the vertical displacement during one actuation cycle, as measured from the four
182 markers identified in Figure 3a. The comparison with the co-plotted voltage signals shows that the
183 displacements had a delay of about 0.5 s. This can be ascribed to a combination of losses derived
184 from the viscosity of the elastomer materials used for the actuator's and cell culture's membranes, as
185 well as the inertia of the coupling fluid between them.



186

187 **Figure 3.** (a) Maximum displacement field map of the cell culture membrane for a sinusoidal voltage
 188 at 4.5 kV and 0.15 Hz; (b) displacement signals captured from the four points identified in (a) during
 189 one actuation cycle; (c) radial and circumferential strains estimated from the four markers shown in
 190 (a). Note: the unexpectedly large radial strain at point D may be due to locally loose constraints close
 191 to that edge, likely to have arisen from manufacturing defects. Error bars represent the standard
 192 deviation among three samples.

193

194 In addition to the vertical displacement, the characterisation included the radial and circumferential
 195 strains. Figure 3c presents their radial distribution, as estimated from the radial and circumferential
 196 displacements of the four markers identified in Figure 3a. The estimation was attained through 3D
 197 reconstructions by processing stereo images of the membrane at resting and deformed states.

198 As expected, both the strains were maximal in the central region of the membrane (about 18% for the
 199 circumferential strain and 15% for the radial strain) and decreased along the radial direction towards
 200 the edge. Nevertheless, it is worth stressing that this preliminary estimate of the strains was limited in
 201 accuracy, as it used only four markers and so the values could not be averaged over a large data set.
 202 This made the values particularly sensitive to defects inevitably introduced during the manual
 203 fabrication of the device, especially at the edges, where the membrane was likely constrained with

204 anisotropic tension. This is evident, for instance, for the radial strain close to the edge (point D in
 205 Figure 3c), whose unexpected high value was probably due to a local loss of tension, possibly
 206 resulting in anomalous bumps.

207 **3.3 Mechanical stimulation of cell cultures**

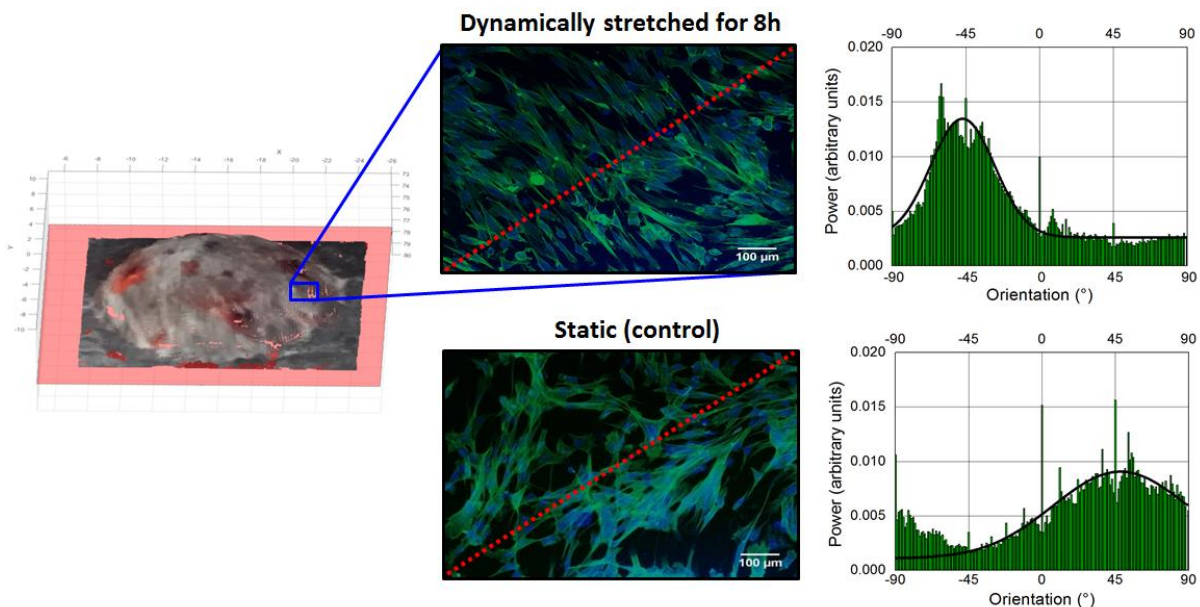
208 In order to verify the bioreactor’s ability to mechanically induce changes on cells adhering to its
 209 surface, the following preliminary tests were conducted (all reagents were purchased from Sigma-
 210 Aldrich).

211 Fibroblasts from the HFFF2 (Human Fetal Foreskin Fibroblasts 2) line were cultured in
 212 supplemented 10% fetal bovine serum DMEM (Dulbecco’s modified eagle medium). Prior to cell
 213 seeding, the cell culture membrane was coated with type I collagen from rat tail. Fibroblasts were
 214 seeded at a density of 100,000 cells per bioreactor well and maintained in a cell culture incubator
 215 (100% humidity, 37 °C, 5% CO₂) for 24 h. Subsequently, the bioreactor was actuated inside the
 216 incubator with a unipolar sinusoidal voltage of 4.5 kV at 0.15 Hz. The stimulation lasted 8 h, which
 217 was considered sufficient to observe morphological changes in the cells, as it is known that
 218 fibroblasts subject to stretch begin to orient within 3 h (Neidlinger-Wilke et al. 2002).

219 The control sample consisted of an identical bioreactor, containing cells with the same passage
 220 number from the same cell batch, cultured in the same conditions, except for cyclic stretching (which
 221 was not performed, as no voltage was applied).

222 At the end of the test, the cells were fixed with 4% paraformaldehyde and stained for actin
 223 (phalloidin) and the nuclei (DAPI). The culture membrane was then imaged at different locations
 224 using a fluorescence microscope (IX81, Olympus, Japan).

225 Figure 4 shows a typical outcome of this test, referring to a portion of the surface located between the
 226 points C and D identified in Figure 3a. Following the stimulation, the cytoskeletal fibers (stained in
 227 green) showed a distinct preferential orientation with respect to those of the control (non-stimulated)
 228 sample.



229

230 **Figure 4.** Effect of cyclic stretching of fibroblasts for 8 h in the bioreactor: images of a cell culture
231 membrane's patch (located between points C and D of Figure 3a), taken from both a dynamically
232 stretched sample, just after stretching, (top) and the static sample of control (bottom). The red dashed
233 lines indicate the radial direction. The graphs next to each image present the angular distribution of
234 the cytoskeletal fibers.

235 In order to quantify this effect, the green-stained fiber alignment was measured via a Fourier
236 component analysis performed by the Directionality plug-in of the Fiji – ImageJ open-source
237 software. The angular orientation of the fibers was computed with respect to a 0° reference defined as
238 the horizontal right-hand direction of the image, with angles increasing counter-clockwise. The
239 results are plotted next to each image in Figure 4: the cells in the stretched sample had a pronounced
240 preferential orientation, with a higher intensity (peaking at -47°) and a narrower dispersion ($\pm 19^\circ$)
241 than those of the control sample (peaking at 48° with a dispersion of $\pm 41^\circ$).

242 This preliminary investigation suggests that the HC-DEA-based bioreactor is able to induce a
243 measurable effect on the orientation of the cytoskeleton and that this orientation tends to be
244 perpendicular to the direction of the imposed radial stretch.

245 A more in-depth assessment of this effect will require systematic testing on a large number of
246 samples, with a diversity of conditions of stimulation, which goes beyond the scope of this Brief
247 Research Report. Nevertheless, it is worth noting that this outcome is in accordance with previously
248 reported findings. Indeed, using other stimulation devices, fibroblasts have been shown to align
249 perpendicularly to the direction of uniaxial cyclic stretch (Huang et al. 2013; Weidenhamer et al.
250 2013). Kang et al. (Kang et al. 2011) suggested that when the actin filaments are cyclically stretched,
251 a perpendicular alignment with respect to the direction of stretch emerges in response to nodal
252 repositioning, to minimize net nodal forces from filament stress states. Similarly, other types of cells,
253 such as lymphatic endothelial cells, have been reported to orient perpendicularly to a uniaxial 10%
254 strain at 0.1 Hz applied for 24 h via a planar DEA-based device (Poulin et al. 2016).

255 Compared to previous studies, the new device proposed here offers a compact and versatile tool for
256 applying strain fields that are not purely uniaxial, nor purely planar, without any additional
257 mechanical equipment. This bioreactor could thus be used to investigate the response of cells
258 stimulated by stretchable substrates undergoing out-of-plane deformations, thereby closer to several
259 conditions *in vivo*.

260 **3.4 Future developments**

261 In addition to systematic testing, future developments should also optimise the actuation elastomer.
262 In this study, the VHB acrylic by 3M was used to facilitate manufacturing, due to its adhesive
263 properties, and take advantage of its high quasi-static electromechanical performance (Pelrine et al.
264 2000). Nevertheless, its high viscosity not only limits the driving frequency to the order of 1 Hz
265 (which however is not a problem for a bioreactor, considering that cells *in vivo* are never exposed to
266 much higher frequencies), but also can cause a significant stress relaxation, especially with the high
267 pre-strains required for optimal operation (Pelrine et al. 2000). Therefore, to avoid a possible
268 reduction of performance over time, less viscous elastomers, like silicones, are a better choice (Maffli
269 et al. 2015; Rosset et al. 2016), enabling devices that should last million cycles (Matysek et al. 2011).

270 Furthermore, improved manufacturing is necessary to reduce manual procedures, which in this work
271 inevitably determined the variability of performance evidenced by the error bars in Figs. 2e and 3.

272 The main drawback of this technology is the need for high voltages (kV), although they have
273 different implications, as discussed below, on the electrical driving units, the cultured cells, the
274 operators and co-located electronics.

275 In terms of driving units, the generation of such voltages is not technically problematic, as the
276 bioreactor does not require high powers and high frequencies. Indeed, the actuator is a capacitive
277 load, which does not absorb high power, and the order of magnitude of frequencies needed for
278 biomimetic cellular stretching is not greater than 1 Hz. For these reasons, in this work it was possible
279 to use the high voltage multiplier by EMCO, which generates up to 5 kV at 0.5 W from an input
280 signal up to 5 V, with a limited bandwidth (about 1 Hz) and a volume of about 2 cm³. Therefore, this
281 kind of bioreactor can be controlled with battery-operated compact units.

282 In terms of interference with cell function, it is worth noting that the culture membrane is not
283 exposed to the high electric field that builds up between the actuation electrodes. Indeed, the main
284 field is confined within the actuation membrane, whilst the fringe field is not expected to impact the
285 cell culture, due to the geometry of the device. In any case, it is useful to consider that previous
286 studies on DEA-based cell stretchers, which have exposed cells to high fringe fields, have not
287 obtained evidence of any effect on cellular (cardiomyocytes) viability (Imboden et al. 2019).

288 In terms of safety for the operators and for electronics which may be connected to the bioreactor (e.g.
289 recording/stimulation electrodes and sensor probes), high voltages introduce the risk of electrostatic
290 discharges (at a low power), which are unpleasant for humans and potentially destructive for
291 electronics. This requires proper insulation of all the high voltage parts, including the voltage
292 multiplier and the leads to the bioreactor. In this work, the high voltage unit was located outside the
293 incubator and had thin cables arranged under the incubator's closed door. As a future simplification,
294 the compact unit could be sealed within the bioreactor's case, obtaining a self-contained system,
295 which could safely be used inside the incubator.

296 So, overall, there are no practical or safety concerns that should discourage the use of this technology
297 just because of the high voltages. Nevertheless, they certainly are a drawback, not only because they
298 bear the risk of electrostatic discharges (e.g. in case of breakdowns), but also because they make the
299 electrical unit bulkier and more expensive than what it could be if the voltages were reduced by one
300 order of magnitude. So, future developments should target a decrease of the voltages to a few
301 hundred Volts. The critical threshold is around 250 V, which is related to low-size and low-cost
302 drivers available for several piezoelectric transducers. To this end, efforts are needed to manufacture
303 reliable DEA membranes with a thickness reduced to a few microns. Although this is challenging,
304 the feasibility has already been proved (Poulin et al. 2015). However, as a lower thickness would
305 reduce the membrane's stiffness, it will be necessary to stack multiple thin dielectric layers
306 intertwined to compliant electrodes, so as to enable both low voltages and adequate stiffness.

307 **4 Conclusions**

308 We described a novel bioreactor to cyclically stretch cells in vitro, via electrically deformable
309 elastomeric membranes with a dynamically tuneable curvature. As compared to state-of-the-art
310 devices, this bioreactor avoids the need for external pneumatic/fluidic drivers or electrical motors,
311 which typically make the whole system bulky and difficult to operate. The electrical tuneability of
312 the membranes is advantageous to obtain compact, self-contained, lightweight and versatile devices.

313 The bioreactor has a modular structure with an interchangeable cell culture unit analogous to that of
314 multi-well plates, enabling the use of standard cell assays.

315 We demonstrated that cyclic stretching for 8 h could induce significant changes in the directionality
316 of fibroblast cytoskeletal fibers, encouraging systematic investigations of this new technology.

317 Although previous studies have already introduced dielectric elastomer actuation for cell stretching,
318 the new configuration described here can generate strain fields that are not purely uniaxial, nor purely
319 planar, but are instead based on the modulation of the cell culture membrane's curvature. This feature
320 opens up new opportunities to exploit this smart-material-based actuation technology to mimic
321 complex 3D deformations occurring in vivo, such as those related to pulmonary inflation, cardiac and
322 vascular pulsation and gastro-intestinal peristalsis.

323 **5 Conflict of Interest**

324 The authors declare that the research was conducted in the absence of any commercial or financial
325 relationships that could be construed as a potential conflict of interest.

326 **6 Author Contributions**

327 F.C., J.C. and M.G. conceived the work. F.C., J.C.B. and A.A. supervised the work. J.C. and M.G.
328 developed the bioreactor and performed the experiments. V.M. and V.F. measured the strains. F.C.
329 and J.C. wrote the paper, with contributions from A.A. and J.C.B.

330 **7 Funding**

331 Financial support is gratefully acknowledged by J. Costa from the company IVTech S.r.l., Italy and
332 by M. Ghilardi from the European MSCA-ITN-2014-Iarie Sklodowska-Curie Innovative Training
333 Network Programme ("MICACT - MICRoACTuators" project, grant agreement 641822).

334 **References**

335 Akbari, S. and Shea, H.R. (2012,a). Microfabrication and Characterization of an Array of Dielectric
336 Elastomer Actuators Generating Uniaxial Strain to Stretch Individual Cells. *Journal of*
337 *Micromechanics and Microengineering* 22 (4): 045020. [https://doi.org/10.1088/0960-](https://doi.org/10.1088/0960-1317/22/4/045020)
338 [1317/22/4/045020](https://doi.org/10.1088/0960-1317/22/4/045020).

339 Akbari, S., and Shea, H.R. (2012,b). An Array of 100 μm ×100 μm Dielectric Elastomer Actuators
340 with 80% Strain for Tissue Engineering Applications. *Sensors and Actuators A: Physical* 186
341 (October): 236–41. <https://doi.org/10.1016/j.sna.2012.01.030>.

342 Balestrini, J. L., Skorinko, J.K., Hera, A., Gaudette, G.R., and Billiar, K.L. (2010). Applying
343 Controlled Non-Uniform Deformation for in Vitro Studies of Cell Mechanobiology. *Biomechanics*
344 *and Modeling in Mechanobiology* 9 (3): 329–44. <https://doi.org/10.1007/s10237-009-0179-9>.

345 Brown, T. D. (2000). Techniques for Mechanical Stimulation of Cells in Vitro: A Review. *Journal of*
346 *Biomechanics* 33 (1): 3–14. [https://doi.org/10.1016/S0021-9290\(99\)00177-3](https://doi.org/10.1016/S0021-9290(99)00177-3).

347 Carpi, F., Frediani, G., De Rossi, D. (2010).Hydrostatically Coupled Dielectric Elastomer Actuators.
348 *IEEE/ASME Transactions on Mechatronics* 15 (2): 308–15.
349 <https://doi.org/10.1109/TMECH.2009.2021651>.

- 350 Carpi, F., De Rossi, D., Kornbluh, R., Pelrine, R., Sommer-Larsen, P. (2008). Dielectric Elastomers
351 as Electromechanical Transducers: Fundamentals, Materials, Devices, Models and Applications of an
352 Emerging Electroactive Polymer Technology. Fundamentals, Materials, Devices, Models and
353 Applications of an Emerging Electroactive Polymer Technology. Oxford: Elsevier, UK.
354 <https://doi.org/10.1016/B978-0-08-047488-5.X0001-9>.
- 355 Carpi, F. (2016). Electromechanically Active Polymers: A Concise Reference. Zurich: Springer
356 International Publishing, Switzerland.
- 357 Cei, D., Costa, J., Gori, G., Frediani, G., Domenici, C., Carpi, F., Ahluwalia, A. (2016). A Bioreactor
358 with an Electro-Responsive Elastomeric Membrane for Mimicking Intestinal Peristalsis.
359 *Bioinspiration & Biomimetics* 12 (1): 16001. <https://doi.org/10.1088/1748-3190/12/1/016001>.
- 360 Clark, W. W., Smith, R., Janes, K., Winkler, J., Mulcahy, M. (2000). Development of a
361 Piezoelectrically Actuated Cell Stretching Device. *Proc. SPIE, Smart Structures and Materials 2000:*
362 *Industrial and Commercial Applications of Smart Structures Technologies*, 3991: 3991–98.
363 <https://doi.org/10.1117/12.388171>.
- 364 Elsaadany, M., Harris, M., Yildirim-Ayan, E. (2017). Design and Validation of Equiaxial Mechanical
365 Strain Platform, EQUicycler, for 3D Tissue Engineered Constructs. *BioMed Research International*
366 2017: 3609703. <https://doi.org/10.1155/2017/3609703>.
- 367 Flexcell International. Online: <https://www.flexcellint.com>. Accessed on October 3, 2019.
- 368 Griffith, L. G. and Swartz, M.A. (2006). Capturing Complex 3D Tissue Physiology in Vitro. *Nature*
369 *Reviews Molecular Cell Biology* 7(3): 211-24. <https://doi.org/10.1038/nrm1858>.
- 370 Han, O., Li, G.D., Sumpio, B.E., Basson, M.D. (1998). Strain Induces Caco-2 Intestinal Epithelial
371 Proliferation and Differentiation via PKC and Tyrosine Kinase Signals. *The American Journal of*
372 *Physiology* 275 (3): 534–41. <https://doi.org/10.1152/ajpgi.1998.275.3.G534>.
- 373 Huang, C., Miyazaki, K., Kaishi, S., Watanabe, A., Hyakusoku, H., Ogawa, R. (2013). Biological
374 Effects of Cellular Stretch on Human Dermal Fibroblasts. *Journal of Plastic, Reconstructive &*
375 *Aesthetic Surgery : JPRAS* 66 (12): e351-61. <https://doi.org/10.1016/j.bjps.2013.08.002>.
- 376 Kang, J., Steward, R. L., Kim, T., Schwartz, R. S., LeDuc, P. R., Puskar, K. M. (2011). Response of
377 an Actin Filament Network Model under Cyclic Stretching through a Coarse Grained Monte Carlo
378 Approach. *Journal of Theoretical Biology* 274 (1): 109–19.
379 <https://doi.org/https://doi.org/10.1016/j.jtbi.2011.01.011>.
- 380 Kim, H. J., Huh, D., Hamilton, G., Ingber, D.E. (2012). Human Gut-on-a-Chip Inhabited by
381 Microbial Flora That Experiences Intestinal Peristalsis-like Motions and Flow. *Lab on a Chip* 12
382 (12): 2165–74. <https://doi.org/10.1039/c2lc40074j>.
- 383 Imboden, M., De Coulon, E., Poulin, A., Dellenbac, C., Rosset, S., Shea, H. & Rohr, S. (2019). High-
384 speed mechano-active multielectrode array for investigating rapid stretch effects on cardiac tissue.
385 *Nature Communications*, 10: 834. <https://doi.org/10.1038/s41467-019-08757-2>.
- 386 Leung, D.Y., Glagov, S., Mathews, M.B. (1977). A New in Vitro System for Studying Cell Response
387 to Mechanical Stimulation. Different Effects of Cyclic Stretching and Agitation on Smooth Muscle

- 388 Cell Biosynthesis. *Experimental Cell Research* 109 (2): 285–98. [https://doi.org/10.1016/0014-4827\(77\)90008-8](https://doi.org/10.1016/0014-4827(77)90008-8).
389
- 390 Maffli, L., Rosset, S., Ghilardi, M., Carpi, F. & Shea, H. (2015). Ultrafast All-Polymer Electrically
391 Tunable Silicone Lenses. *Adv. Funct. Mater.* 25: 1656–1665.
392 <https://doi.org/10.1002/adfm.201403942>.
- 393 Matysek, M., Lotz, P., Schlaak, H. F. (2011). Lifetime investigation of dielectric elastomer stack
394 actuators. *IEEE Transactions on Dielectrics and Electrical Insulation*, 18(1): 89-96.
395 <https://doi.org/10.1109/TDEI.2011.5704497>.
- 396 Meikle, M. C., Reynolds, J.J., Sellers, A., Dingle, J.T. (1979). Rabbit Cranial Sutures in Vitro: A
397 New Experimental Model for Studying the Response of Fibrous Joints to Mechanical Stress.
398 *Calcified Tissue International* 28 (2): 137–44. <https://doi.org/10.1007/bf02441232>.
- 399 Neidlinger-Wilke, C., Grood E., Claes, L., Brand, R. (2002). Fibroblast Orientation to Stretch Begins
400 within Three Hours. *Journal of Orthopaedic Research* 20 (5): 953–56. [https://doi.org/10.1016/S0736-0266\(02\)00024-4](https://doi.org/10.1016/S0736-0266(02)00024-4).
- 402 Pavesi, A., Adriani, G., Rasponi, M., Zervantonakis, I.K., Fiore, G.B., Kamm, R.D. (2015).
403 Controlled Electromechanical Cell Stimulation On-a-Chip. *Scientific Reports* 5 (July): 11800.
404 <http://dx.doi.org/10.1038/srep11800>.
- 405 Pelrine, R., Kornbluh, R., Pei, Q. & Joseph, J. (2000) High-Speed Electrically Actuated Elastomers
406 with Strain Greater Than 100%. *Science* 287, 836–839.
407 <https://doi.org/10.1126/science.287.5454.836>.
- 408 Poulin, A., Demir, C.S., Rosset, S., Petrova, T. V., Shea, H. (2016). Dielectric Elastomer Actuator for
409 Mechanical Loading of 2D Cell Cultures. *Lab on a Chip* 16 (19): 3788–94.
410 <https://doi.org/10.1039/C6LC00903D>.
- 411 Poulin, A., Imboden, M., Sorba, F., Grazioli, S., Martin-Olmos, C., Rosset, S., Shea, H. (2018). An
412 Ultra-Fast Mechanically Active Cell Culture Substrate. *Scientific Reports* 8 (1): 9895.
413 <https://doi.org/10.1038/s41598-018-27915-y>.
- 414 Poulin, A., Rosset, S. & Shea, H. R. (2015) Printing low-voltage dielectric elastomer actuators. *Appl.*
415 *Phys. Lett.* 107: 244104. <https://doi.org/10.1063/1.4937735>.
- 416 Rosset, S. & Shea, H. R. (2016). Small, fast, and tough: Shrinking down integrated elastomer
417 transducers. *Appl. Phys. Rev.* 3: 031105. <https://doi.org/10.1063/1.4963164>.
- 418 Saul, J.P. (1990). Beat-To-Beat Variations of Heart Rate Reflect Modulation of Cardiac Autonomic
419 Outflow. *Physiology* 5 (1): 32–37. <https://doi.org/10.1152/physiologyonline.1990.5.1.32>.
- 420 Strex Inc. Online: <https://strexcell.com>. Accessed on October 3, 2019.
- 421 Taylor, J. A. and Eckberg, D.L. (1996). Fundamental Relations Between Short-Term RR Interval and
422 Arterial Pressure Oscillations in Humans. *Circulation* 93 (8): 1527–1532.
423 <https://doi.org/10.1161/01.cir.93.8.1527>

424 Weidenhamer, N. K. and Tranquillo, R.T. (2013). Influence of Cyclic Mechanical Stretch and Tissue
425 Constraints on Cellular and Collagen Alignment in Fibroblast-Derived Cell Sheets. *Tissue*
426 *Engineering. Part C, Methods* 19 (5): 386–95. <https://doi.org/10.1089/ten.TEC.2012.0423>.